







# Seismic Performance of Dual-Concentrically Braced Frames with Slim-Floor Beam-to-Column Joints

Rafaela Don<sup>1,3</sup> , Cristian Vulcu<sup>1,3</sup> , Adrian Ciutina<sup>2</sup> ,  
and Aurel Stratan<sup>1</sup> 

<sup>1</sup> Department of Steel Structures and Structural Mechanics,  
Politehnica University Timisoara, Timisoara, Romania  
aurel.stratan@upt.ro

<sup>2</sup> Department of Overland Communication Ways, Foundation and Cadastral  
Survey, Politehnica University Timisoara, Timisoara, Romania  
adrian.ciutina@upt.ro

<sup>3</sup> Institute of Steel Construction, RWTH-Aachen University, Aachen, Germany  
{r.don, c.vulcu}@stb.rwth-aachen.de

**Abstract.** Due to architectural advantages and, more recently demonstrated, to the applicability to seismic design, the slim-floor moment-resisting beam-to-column joints could be an efficient solution to mid- and high-rise structures. The integration of the slim-floor beam into relatively tall steel and composite structures designed to withstand inertial forces caused by seismic action was achieved on a two-dimensional Dual-Concentrically Braced Frame system. The central focus of the study is the seismic performance evaluation of this frame with nonlinear static and dynamic analyses. The analyses' results evidenced an adequate seismic performance, proof of which were the following: damage sustained at each Limit State, progressive development of plastic mechanisms, limited inter-storey drifts and maximum joint rotation demand lower than experimentally proven. These results demonstrate the possibility of using slim-floor beam-to-column joints in seismic-resistant structures.

**Keywords:** Slim-floor beam-to-column joint · D-CBF · Seismic performance

## 1 Introduction

The slim-floor (*SF*) system is best applicable to mid- to high-rise steel and composite structures, as it allows for enhanced architectural freedom due to floor thickness reduction and possible additional storeys [1]. Usually, a seismic and cost-efficient design of tall structures is achieved by combining braced and unbraced structural systems (i.e., Dual Frames). This approach provides control on the development of the global mechanism by limiting inter-storey drifts and ensuring seismic energy dissipation through plastic deformations [2, 3]. Although the application of the *SF* system to multi-storeys structures is no longer a novelty in civil engineering, a different objective for this flooring configuration was recently proposed [4, 5], where instead of using the *SF* in the gravity load-resisting system in the form of simply-supported beams [6], it is

integrated in the lateral load-resisting system by using moment-resisting beam-to-column joints. This study on Moment-Resisting Frames (MRFs) was previously published [7]. The seismic design of MRFs relies on the strong column–weak beam concept, which forces the inelastic deformations development in the beams [8]. This requires the beam to possess the ability to dissipate seismic energy. A brief joint design approach and detailing can be found in [9]. As the use of the rigidly-connected *SF* beam as a dissipative structural element was demonstrated with cyclic tests on beam-to-column joint specimens [5], the applicability of the solution to multi-storey structures prone to seismic hazard is justified. Experimentally, the joint assemblies developed high flexural resistance and stiffness in hogging and sagging bending and attained a cyclic rotation capacity of  $\pm 43.4$  mrad at Significant Damage (SD), fulfilling the AISC 341-10 requirement [10]. Thus, the aim of the current study was to assess and prove the seismic performance of a Dual Concentrically-Braced Frame (D-CBF) with MRF sub-systems that contain *SF* beams through nonlinear static and dynamic analyses.

## 2 Dual Concentrically-Braced Frame: General Aspects

The D-CBF was developed and analysed in plane with Sap2000 [11] and incorporated MRF bays adjacent to a central CBF bay (see figure from Table 1). The analysed frame was part of the lateral load-resisting system whose position was on the perimeter of a three span-by-three bay floor layout (in total:  $18 \times 18$  m). In elevation, the mid-rise frame of the office building included 16 storeys of 3.2 m in height. The following loads were applied: permanent on floors  $5 \text{ kN/m}^2$  and on perimeter beams (from the facade)  $3.2 \text{ kN/m}$ ; live  $3.8 \text{ kN/m}^2$ ; seismic:  $a_g = 0.3 \cdot g$ /soil type C. Gravity loads acting on the gravity load-resisting system were assigned to a leaning column.

The design of the structural elements was carried out in accordance with the specific rules of Ductility Class 3 of prEN 1998-1-2 [8]. The followings boundary conditions were applied: fixed column base, rigidly-connected *SF* beam (in accordance with the tested beam-to-column joint assembly shown in Table 1 and [9]) and rigid diaphragm at each storey to account for the concrete slab in-plane effect. As capacity design was applied, the structural elements were divided into dissipative (i.e., braces, *SF* beams, column bases eventually) and non-dissipative (i.e., columns, connections) components. The *SF* beams were modelled considering their geometrical (“full” section, dissipative zone with *Reduced Flange Section – RFS* [9]) and mechanical particularities ( $I_{eq}$ ) as shown in [7]. The “X” braces spanned over two storeys and were modelled with pinned ends. The brace design and verification in the linear static analysis were performed with prEN 1998-1-2 [8] and prEN 1993-1-1 [12]. According to the code [8], the upper limit value of the behaviour factor  $q$  for a Dual Frame could be considered 4.8, provided that the contribution of the MRF sub-systems to the total resistance was at least 25%. This verification was carried out with nonlinear analyses and confirmed a contribution of the MRFs of 25% at Damage Limitation and 35% at Significant Damage. The linear static analysis revealed that the design was governed by resistance and that the D-CBF was not susceptible to second-order effects. To optimise the steel consumption and to avoid a relatively long period of vibration, an outrigger

belt truss was positioned at the 16<sup>th</sup> floor. The resulted cross-sections with the corresponding steel grade, as well as the fundamental period of vibration are shown in Table 1.

**Table 1.** Overview: joint/brace configuration, structural system (D-CBF), cross-sections.

<ul style="list-style-type: none"> <li>▪ Belt truss (S355), CHS Braces (S275), Columns (S355)</li> <li>▪ Beams: fixed SF beam (½ IPE600 + Pl. 380×20, S355) [5]</li> </ul>		Outer / Inner	CHS Braces	
		Flr. Columns	(flr. 1÷15)	
		16	HE 360 B	HE 200 B
		15	HE 360 B	114.3 x 5.0
		14	HE 360 B	114.3 x 6.3
		13	HE 360 B	133.0 x 6.0
		12	HE 360 B	133.0 x 6.3
		11	HE 360 B	139.7 x 6.0
		10	HE 450 B	139.7 x 6.0
		9	HE 450 B	139.7 x 7.1
		8	HE 500 B	139.7 x 7.1
		7	HE 500 B	159.0 x 6.3
		6	HE 600 B	159.0 x 6.3
		5	HE 600 B	168.3 x 8.0
		4	HE 600 B/M	168.3 x 7.1
		3	HE 600 B/M	168.3 x 10
		2	HE 700 B/M	168.3 x 8.0
		1	HE 700 M	168.3 x 7.1

### 3 Seismic Performance Assessment

#### 3.1 Definition of the Nonlinear Behaviour

The nonlinear behaviour of the *SF* beams was defined through plastic hinges for members subjected to flexure. The backbone curve characterised the dissipative zone of the *SF* beam and accounted for the presence of the concrete slab (see joint assembly in Table 1). The backbone curve was obtained from cyclic tests on *SF* joint assemblies [5] and was introduced in the software as shown in [7]. The nonlinear column behaviour was defined through a plastic hinge for members subjected to axial loading with flexure and through a backbone curve from FEMA 356 [13].

As the braces have major role in the development of the global plastic mechanism and in the seismic performance of the D-CBF, the accuracy of their numerical modelling played a central role. The numerical model of the braces was adapted to the nonlinear analysis type. The inelastic brace behaviour was defined through an axial force-axial deformation phenomenological model (*P hinge*) and the acceptance criteria from FEMA 356 [13] were adopted in the nonlinear static analyses. Under compression, the plastic deformations at Damage Limitation (DL), Significant Damage (SD) and Near Collapse (NC) were defined as  $0.25\Delta_c$ ,  $4\Delta_c$  and  $6\Delta_c$ . Under tension, the

plastic deformations at DL, SD and NC were defined as  $0.25\Delta_t$ ,  $7\Delta_t$  and  $9\Delta_t$ . Whereas  $\Delta_c$  is the axial deformation at the anticipated buckling load,  $\Delta_t$  is the axial deformation at the anticipated tensile yielding load.

Following recommendations from literature [14], the hysteretic response of the braces was defined by modelling each brace with two physical theory models (*P-M2-M3 fibre plastic hinge*) and adding an initial imperfection in nonlinear dynamic analyses. Moreover, the cross-section contained 100 fibres, two fibres being added on the thickness of the CHS braces. The same acceptance criteria of FEMA 356 [13] were considered for physical theory model under compression/tension, as for the phenomenological model. The outcomes from each plastic hinge (i.e. “axial force vs. axial deformation curve” and “bending moment vs. rotation curve”) were manually post-processed to obtain the “force-deformation curve” corresponding to each brace. The maximum deformations were compared to the acceptance criteria corresponding to braces under compression/tension from FEMA 356 [13], rated and marked accordingly on the structure (see Fig. 2d). The nonlinear modelling and post-processing procedures of the braces were verified by comparison to the experimental data from a cyclic test performed on a double pinned CHS brace (i.e., SP59-1 [15]).

### 3.2 Outcomes from the Nonlinear Static and Dynamic Analyses

From the nonlinear static analysis, a capacity curve was obtained for the D-CBF structure. Further, the target displacements ( $D_t$ ) corresponding to the three seismic intensity levels were computed using the N2 method [16] (DL with the ratio between PGA and reference-PGA  $a_g/a_{gr} = 0.5$ ; SD with  $a_g/a_{gr} = 1.0$ ; and NC with  $a_g/a_{gr} = 1.5$ ):  $D_{t,DL} = 0.25$  m,  $D_{t,SD} = 0.50$  m,  $D_{t,NC} = 0.75$  m. The target displacements are marked on the capacity curve shown in Fig. 1a, while the damage state of the D-CBF shown in Fig. 1b evidenced the following:

- at DL seismic intensity: an elastic response of the structure, except for seven compressed braces which sustained deformations consistent with DL and three other compressed braces with pre-DL deformations;
- at SD seismic intensity: a wide distribution of plastic hinges was evidenced in the braces; the nonlinear response of most braces was activated, the deformations corresponding mainly to DL. Three compressed braces located in the middle of the structure attained SD deformations; one brace attained NC deformations. The *SF* beams from the third to the tenth storeys reached pre-DL rotations. No plastic hinges were developed in columns.
- at NC seismic intensity: the compressed braces attained deformations ranging from DL to NC, while most tensioned braces developed deformations associated with DL. The *SF* beams sustained rotations associated with DL. No evidence of plastic hinge development was found in the columns.

Based on the nonlinear static analysis and on the N2 method [16] results, the D-CBF evidenced an adequate seismic performance. Apart from the damage state of the D-CBF structure at the three Limit States, proof of this were also the reduced inter-storey drifts. For instance, the maximum inter-storey drifts were: 6.7 mrad at DL;

17 mrad at SD; and 28.2 mrad at NC. Neither of these values exceeded the imposed criteria of 7.5 mrad at DL and 20 mrad at SD [8] for Dual Frames.

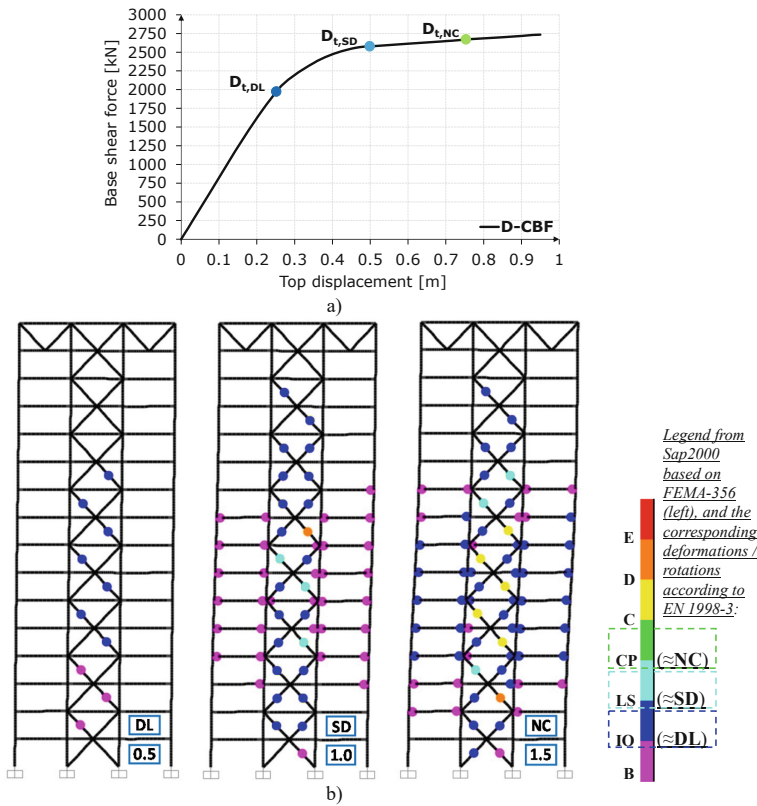


**Fig. 1.** Nonlinear static analysis: a) capacity curve; b) response at DL, SD & NC intensity levels

The assessment of the seismic performance of the D-CBF was completed with Response History Analyses (RHA), which are more appropriate for medium/high-rise buildings. For this purpose, a set of seven semi-artificial accelerograms matching the target spectrum and meeting the criteria [8] was selected and generated [17]. Further details regarding the accelerograms are available in [7]. Some of the RHA outcomes are shown in Fig. 2a–d for the most detrimental accelerogram (i.e., #A3 [7]) in terms of: (i) displacement at the top floor; (ii) damage state of the D-CBF at the DL, SD and NC seismic intensity levels. Accelerogram #A3 is depicted as the most detrimental, as it produced more structural damage than the others from the applied set.

- DL seismic intensity. The results at DL seismic intensity proved an elastic response of the structure. While some of the compressed braces attained DL deformations, the rest of the structure remained in the elastic range. Apart from that, no residual deformations were evidenced (see Fig. 2a).

- **SD seismic intensity.** At SD seismic intensity, an even distribution of plastic hinges was evidenced in the braces; while most of them developed plastic hinges with deformations associated mainly to DL, a few compressed braces attained SD deformations. The *SF* beams from the middle section of the frame reached pre-DL rotations (floors 4÷12). However, no plastic hinges were developed in the columns. As shown in Fig. 2b, some residual deformations were recorded.
- **NC seismic intensity.** As the global plastic mechanism developed at NC seismic intensity, many of the compressed braces reached deformations associated with LS or even NC. Only two braces attained deformations that exceeded NC. On the other hand, all tensioned braces (having the main role within the lateral load-transfer mechanism) developed DL or SD deformations. Most *SF* beams attained DL rotations and plastic hinges were developed at two column bases. Higher residual deformations were recorded (see Fig. 2c).

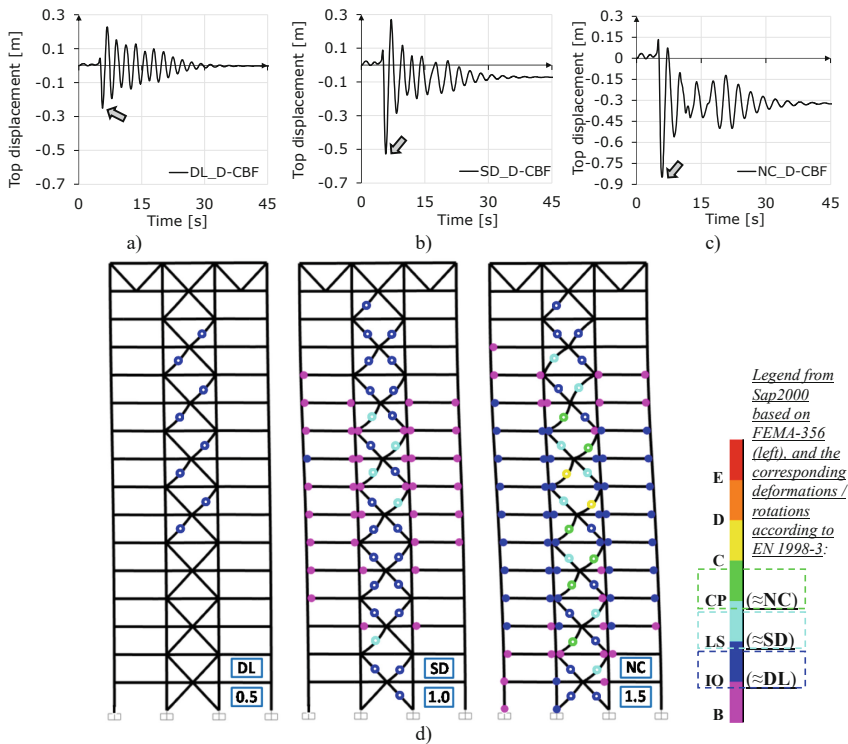


**Fig. 2.** Response History Analyses outcomes corresponding to accelerogram #A3 at DL/SD/NC seismic intensity levels: a) b) c) displacement at the top floor; d) damage state

In addition to the global plastic mechanism, the seismic response was also evaluated in terms of storey deformations. The inter-storey drifts on the height of the analysed frame are illustrated in Fig. 3a–b in two different scenarios: (i) maximum drift

values generated by accelerogram #A3 and (ii) mean values obtained from all accelerograms (#A1÷A7). The drift values are also centralised in Table 2. As can be observed, the mean inter-storey drifts respected the imposed criterion at DL and SD limit states.

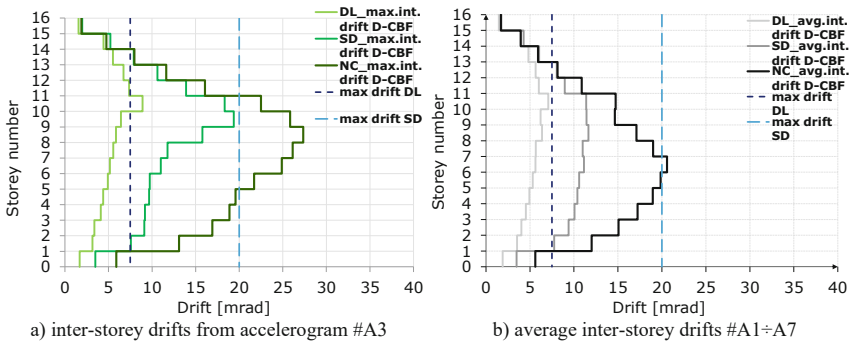


**Fig. 3.** Response History Analyses – inter-storey drift values: a) maximum; b) average

**Table 2.** Inter-storey drifts from Response History Analyses: *maximum* and average values

Limit states	<i>Maximum drifts (#A3)</i>	<i>Average drifts (#A1÷A7)</i>
Damage Limitation (DL)	8.9 mrad	7.1 mrad
Significant Damage (SD)	19.4 mrad	11.7 mrad
Near Collapse (NC)	27.3 mrad	20.6 mrad

## 4 Conclusions

The current paper presents the seismic performance evaluation of a 16-storey Dual-Concentrically Braced Frame (D-CBF) with nonlinear static and dynamic analyses. The analysed D-CBF included: (i) a central bay with X-braces spanning over two storeys – representing the CBF sub-system and (ii) two adjacent bays containing moment-resisting slim-floor beam-to-column joints – as the MRF sub-systems. The nonlinear definitions of the *SF* beams [5] and the braces [15] were based on experimental tests. Thus, the numerical *SF* beam model contained the “real” geometrical characteristics, a computed equivalent second moment of inertia  $I_{eq}$  and a backbone curve obtained from the cyclic tests on joint assemblies with concrete slab. Depending on the analysis, two nonlinear brace models were used: phenomenological and physical theory. Both models were compared to the response of a tested brace specimen. They also followed the recommendations of [14] and complied with [13].

The analysis results proved an adequate seismic performance of the D-CBF, proof of which were: ■ the sustained damage at each Limit State; ■ the sequence in which the plastic hinges developed and the obtained global plastic mechanism (see Fig. 1b, Fig. 2d); ■ the limited inter-storey drifts. This is also supported by the maximum inter-storey drift demand at SD intensity level: 17 mrad (Pushover), 11.7 mrad (Response

History Analysis). Experimentally, the rotation capacity of the *SF* beam-to-column joint at SD was  $\pm 43.4$  mrad [5], which is higher than the demand. The contribution of the MRF sub-systems to the total resistance of the D-CBF was verified and found satisfactory (see Sect. 2). Based on these results, it can be concluded that moment-resisting *SF* beam-column joints are applicable to seismic-resistant structural systems.

**Acknowledgements.** The 2<sup>nd</sup> author was supported by the Alexander von Humboldt Foundation through a Research Fellowship for Experienced Researchers. This support and the hospitality provided by RWTH-Aachen University/CWE are hereby gratefully acknowledged.

## References

1. ArcelorMittal (2017) High-rise buildings (brochure). Long Prod. Sect. & Merchant Bars
2. Dubina D, Dinu F, Stratan A (2009) Tower centre international building in Bucharest. Part I: structural design. *Steel Constr* 2(4):256–263
3. Dubina D, Dinu F, Stratan A (2021) Resilience of steel-dual frame buildings in seismic areas. *Steel Constr* 14(3):150–166
4. Yang L, Wang Y, Shi Y (2015) Full-scale test of two-storey composite slim floor under pseudo-dynamic and pseudo-static loadings. *Adv Struct Eng* 18(2):173–188
5. Don R, Ciutina A, Vulcu C, Stratan A (2020) Seismic-resistant slim-floor beam-to-column joints: experimental and numerical investigations. *JSCS* 37(3):307–321
6. Hauf G (2010) Trag- und Verformungsverhalten von Slim-Floor Trägern unter Biegebeanspruchung. Ph.D. thesis. Univ. Stuttgart, Institut für Konstruktion und Entwurf, Stuttgart, Germany. ISSN 1439-3751, D 93
7. Don R, Ciutina A, Stratan A, Vulcu C (2021, in press) Slim-floor beam-to-column joints for seismic-resistant structures: joint performance and case study on MRFs. In: 9th International conference composite construction in steel and concrete. Ernst & Sohn, Stromberg, Germany
8. CEN: Eurocode 8: Design of structures for earthquake resistance - Part 1-2: Design of structures for earthquake resistance. Brussels, Belgium (EN 1998-1-2:2020, draft)
9. Don R, Vulcu C, Ciutina A, Stratan A (2022, in press) Slim-floor beam-to-column joints for seismic-resistant structures: design approach & detailing. In: 10th international conference on the behaviour of steel structure in seismic areas, Timisoara, Romania
10. AISC (2010) Seismic provisions for structural steel buildings. AISC 341, Chicago, USA
11. CSI Berkley (2019) SAP2000 v21. Copyright Computers and Structures
12. CEN: Eurocode 3: Design of steel structures - Part 1-1: General rules and rules for buildings. Brussels, Belgium (EN 1993-1-1:2020, draft)
13. FEMA 356 (2000) Prestandard and commentary for the seismic rehabilitation of buildings. Federal Emergency Management Agency, Washington, D.C.
14. D’Aniello M, La Manna Ambrosino G, Portioli F, Landolfo R (2013) Modelling aspects of the seismic response of steel concentric braced frames. *JSCS* 15(5):539–566
15. Gabor G et al (2012) Experimental & numerical validation of the technical solution of a brace with pinned connections for seismic-resistant multi-story structures. In: 15th world conference on earthquake engineering, Lisbon, Portugal, paper 4431, 24–28 September 2012
16. Fajfar P (2000) A nonlinear analysis method for performance-based seismic design. *Earthq Spectra* 16(3):573–592
17. Akkar S et al (2014) Reference database for seismic ground-motion in Europe (RESORCE). *Bull Earthq Eng* 12(1):311–339. <https://doi.org/10.1007/s10518-013-9506-8>